IAF-89-270

IAF

MARS ROVER RTG STUDY

Principal Investigator & Author:

A. Schock

Contributors:

T. Hamrick
T. Or
V. Sankarankandath
M. Shirbacheh (JPL)
E. Skrabek

Fairchild Space Company
20301 Century Boulevard
Germantown, Maryland 20874
United States of America

40th CONGRESS OF THE INTERNATIONAL ASTRONAUTICAL FEDERATION

October 7-13, 1989/Torremolinos, Malaga-Spain

MARS ROVER RTG STUDY

A. Schock, T. Hamrick, T. Or, V. Sankarankandath, E. Skrabek
Fairchild Space Company, Germantown, MD

M. Shirbacheh
Jet Propulsion Laboratory, Pasadena, CA

ABSTRACT

The paper describes the design and analysis of Radioisotope Thermoelectric Generators (RTGs) for powering the Mars Rover vehicle, which is a critical element of the unmanned Mars Rover and Sample Return mission (MRSR). The RTG design study was conducted by Fairchild Space Company for the U.S. Department of Energy, in support of the Jet Propulsion Laboratory's MRSR project.

The paper briefly describes a reference mission scenario, an illustrative Rover design and activity pattern on Mars, and its power system requirements and environmental constraints, including the RTG cooling requirements during transit to Mars. It identifies the key RTG design problem, i.e. venting the helium generated by the fuel's alpha decay without intrusion of the Martian atmosphere into the RTG, and proposes a design approach for solving that problem. Using that approach, it describes and analyzes a variety of RTG designs, all based on the proven and safety-qualified General Purpose Heat Source module.

The first RTG option described is a very conservative baseline design, employing standard thermoelectric unicouples whose reliability and performance stability has been extensively demonstrated on previous space missions. The heat source of the 250-watt RTG consists of a stack of 18 separate modules that is supported at its ends but not along its length. The paper describes and analyzes the structure that holds the stack together during Earth launch and Mars operations, but allows it to come apart in case of an inadvertent reentry.

It then summarizes the baseline RTG's mass breakdown, and presents a detailed description of its thermal, thermoelectric, and electrical analyses. It examines the effect of different operating conditions (beginning versus end of mission, water-cooled versus radiation-cooled, summer day versus winter night) on the RTG's performance. Finally, the paper compares the RTGs' specific powers for different power levels (250W versus 125W), different thermoelectric element designs (standard versus short unicouples versus multicouples) and different thermoelectric figures of merit ($0.00058K^{-1}$ to $0.00140K^{-1}$).

The results presented show the RTG performance achievable with current technology, and the performance improvements that would be achievable with various technology developments. It provides a basis for selecting the optimum strategy for meeting the Mars Rover design goals with minimal programmatic risk and cost.

1.0 SCOPE AND OBJECTIVES OF STUDY

In December 1988 the U.S. Department of Energy's Office of Special Applications (DOE/OSA) asked Fairchild Space Company to investigate RTG (Radioisotope Thermoelectric Generator) design options for powering a Martian Rover vehicle. That vehicle is a critical part of the Mars Rover and Sample Return (MRSR) mission, which is under preliminary study by NASA's Jet Propulsion Laboratory (JPL) with the support of the Johnson Space Center (JSC). JPL is responsible for the overall MRSR study and, among other items, for the design of the Rover vehicle.

The purpose of the DOE-sponsored Fairchild study is to support JPL and JSC by providing the mission planners with information about the RTG masses and sizes for a conservative baseline design and for various options of differing technology readiness. One of the primary aims of the study is to quantify the performance improvements achievable if new technologies are successfully developed, to estimate the required time, effort, success probability, and programmatic risk in developing those new technologies, and thus to help identify the best strategy for meeting the MRSR system goals.

In addition, the Fairchild study is useful in specifying critical design and operational requirements for integrating the RTG with the Rover and the launch vehicle (particularly cooling during orbit transfer), and in identifying what additional information JPL and JSC will need to furnish before the RTG design can be finalized.

This paper presents an abbreviated description of the study and its results. A much fuller description is contained in a Fairchild report [1], available from the author.

2.0 MISSION

2.1 BACKGROUND

The long-term goal of the National Aeronautics and Space Administration is to expand human presence beyond Earth and into the Solar System [2]. Mars, with its potential for eventual habitability, is targeted for human exploration and colonization. A manned mission to Mars must be preceded by robotic exploration of Mars, to bridge the gap between the knowledge gained by the 1976 Viking Mission and the knowledge required for a safe and effective human journey to Mars.

The Jet Propulsion Laboratory and Johnson Space Center are jointly studying such a mission, called Mars Rover Sample Return. That study is focused on understanding the system requirements and generating the first-order system design that meets these requirements [3]. The mission requires orbiters, landers and a Rover in Mars orbit and/or on the Mars surface.

RTGs have been selected as the primary power source for the surface elements of the MRSR system. They have a long and successful history of space flight, and their reliability and performance have been demonstrated in missions such as Pioneer, Viking, and Voyager [4]. The current-generation RTGs, however, are designed for space operation and must be modified for Mars surface operation.

2.2 MRSR OBJECTIVES AND SYSTEM ELEMENTS

The objective of the MRSR mission is to determine the geological, climatological and biological history of the planet Mars, and to characterize its near-surface materials. The mission will also provide information on the Mars environment, and test key technologies for human exploration of the planet. The mission objectives are achieved by making in-situ analyses and returning selected samples to Earth for extensive studies.

A spectrum of possible mission and system designs has been examined against the broad science requirements [5]. These missions, which varied in launch configuration, launch date, and the various elements that constitute the mission, have been narrowed down to a reference mission that consists of five system elements: an Imaging Orbiter (IO), Communications Orbiter (CO), Rover, Sample Return Orbiter (SRO) and Mars Ascent Vehicle (MAV). The reference MRSR mission scenario and possible timeline envisioned by the JPL project team is summarized in Figure 1 and in the following paragraphs. As shown, the five system elements under this scenario are launched in four separate launch segments.

The Imaging Orbiter is launched aboard a Titan IV/IUS in October-November 1996, with Mars arrival in August-October of 1997. It maps the surface of the planet within 39 degrees of the Martian equator for landing site selection and Rover Traverse Planning [6]. A total of ten 10 x 10 km sites are mapped for selection of the landing site, and an area of 20 x 20 km at that site is more finely mapped for Rover Traverse planning.

The Communication Orbiter provides the communication link between the Mars surface elements and Earth [6]. It is launched in November-December 1998 aboard a Titan IV/IUS, and is placed in a stationary orbit such that the region between 65.7^{o} south and north of the equator is covered continuously. The Rover-to-Earth link is available at least 95% of every Mars Sol.

The Rover element is launched aboard a Titan IV/Centaur in December 1998, with arrival at Mars in October 1999-January 2000. The Rover traverses the surface of Mars, performs in-situ analyses, deploys science packages, selects samples and returns them to the ascent vehicle for delivery to Earth. Right after its arrival, the images transmitted by the Rover are used to select a landing site for the MAV. The Rover design and its requirements are described in more detail in the next section.

The Sample Return Orbiter (SRO) and Mars Ascent Vehicle (MAV) are launched together onboard a Titan IV/Centaur in December 1998-February 1999, with arrival on Mars in October 1999-February 2000. The SRO/MAV flight segment is aerocaptured into a circular orbit around Mars [7]. After site certification by the Rover, the MAV descends to the Mars surface, where it deploys a meterological-geophysical science package and collects contingency samples from its local environment. The SRO remains in orbit awaiting the return of the MAV and the Mars samples. The Rover transfers its collected samples to the MAV from time to time, until MAV's ascent from the Mars surface around December 2000. After liftoff from Mars, the MAV docks with the SRO and transfers the collected samples to it. The Earth return vehicle is then separated from the SRO to bring the samples back for aerocapture into low-Earth orbit, where its Martian samples are picked up by the shuttle.

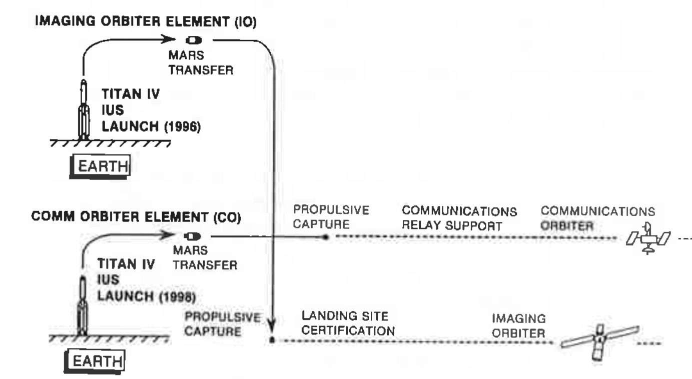

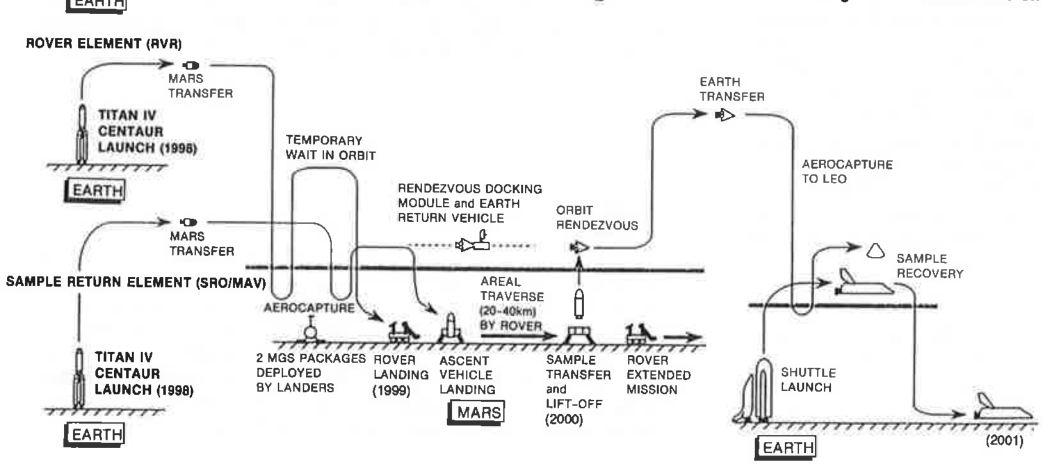

Figure 1. MRSR Reference Mission Scenario

2.3 MARS ROVER

The Rover element of the Mars Rover Sample Return mission for which the RTG study was performed is required to traverse more than 40 kilometers and collect 100 samples from several geologically distinct sites [8]. The Rover is equipped with semi-autonomous navigation capability, which means it can compare its surroundings with a stored map of the orbital view obtained by the Imaging Orbiter, and plan and execute a local path toward a designated point. This autonomy greatly increases the Rover's range, since it reduces the need for frequent commands from Earth. Theoretically, the Rover can go several kilometers without requiring intervention from Earth.

The Rover returns with samples to the Mars Ascent Vehicle (MAV) several times. Each time the distance traveled expands as the confidence in the Rover is increased. A typical activity pattern is depicted in Figure 2.

Figure 2. Illustrative Rover Activity Pattern

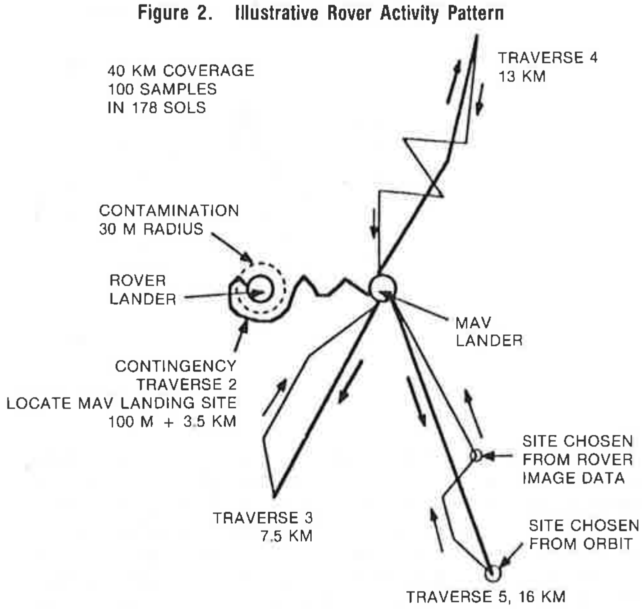

The Rover is equipped with an imaging camera, multispectral imaging instruments for science and navigation, optical microscope, spectrometers (alpha, proton, neutron, x-ray), electromagnetic sounders, gas analyzer, and differential scanning calorimeter. The sample acquisition by the Rover is accomplished in several stages: remote sample characterization, location and designation of interesting samples, positioning and manipulation of the Rover to acquire the sample, and preserving the samples for return to the MAV.

Several different Rover designs and mobility systems are under investigation. One possible mobility system is illustrated in Figure 3. It employs a six-wheeled pantograph, with one-meter wheels that can move across rough terrain. This design was developed by a JPL in-house study.

An alternative Rover design is illustrated in Figure 4. This "walking beam" design was developed by the Martin Company, under contract to JPL. In the illustrated version, it employs two tripods, linked by a tracked beam. During movement, one tripod rests on the ground, and the legs of the other are raised, enabling it to move along the tracked beam. During the next step, the position of the two tripods are reversed. Directional changes are accomplished by using a turntable to pivot the raised tripod about the point where it joins the grounded tripod.

Figure 3. Illustrative Rover Design: Wheeled-Vehicle Option

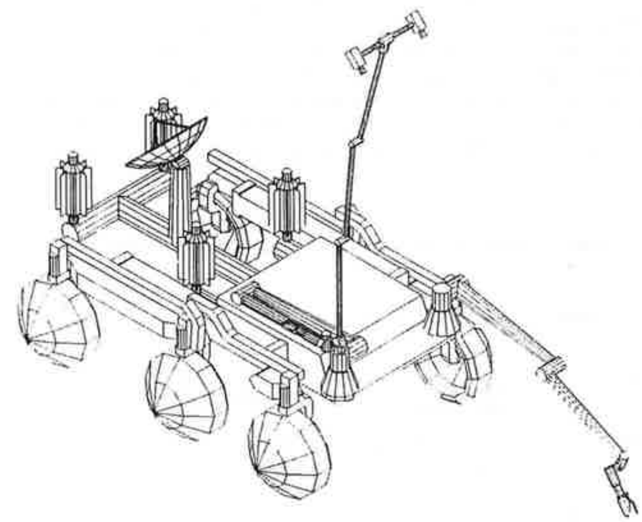

Figure 4. Illustrative Rover Design: Walking-Beam Option

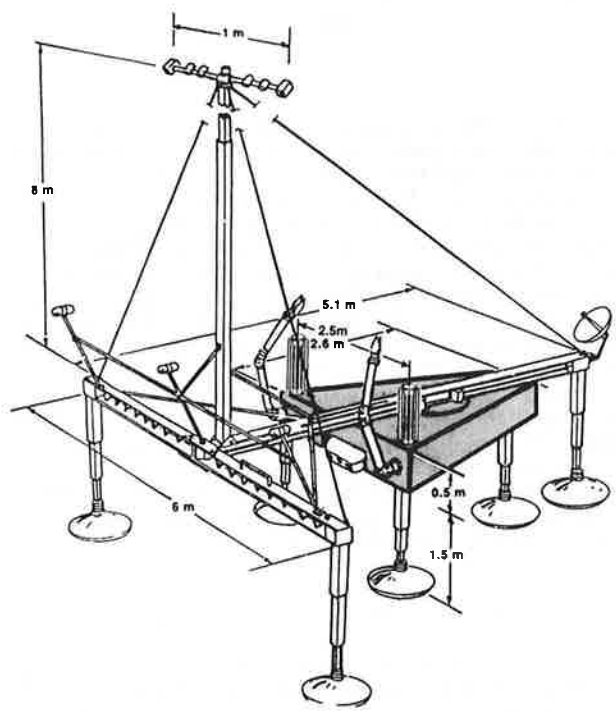

3.0 ROVER POWER SYSTEM

3.1 RTG REQUIREMENTS

The MRSR mission calls for the Rover to operate for four years after launch. The launch is assumed to occur three years after fuel encapsulation, and to be preceded by one year of full-temperature operation of the thermoelectric converters. Thus, by the end of the mission the RTG's fuel will have decayed for seven years, and its converters will have degraded as a result of operating at full temperature for five years.

As illustrated in Figure 5, the Rover has an average power requirement of 500 watts, with peak power demands of over one kilowatt when the Rover is climbing a slope or in the process of sample acquisition. The RTGs will be designed to provide continuous power with an output of 500 watts at the end of the mission, and will be supplemented by high-power-density rechargeable batteries for meeting power demand peaks that exceed the output of the RTGs. These batteries will be recharged by the RTGs during periods of low power demand.

Figure 5. Power Demand Profile for Typical Mars Rover Activities

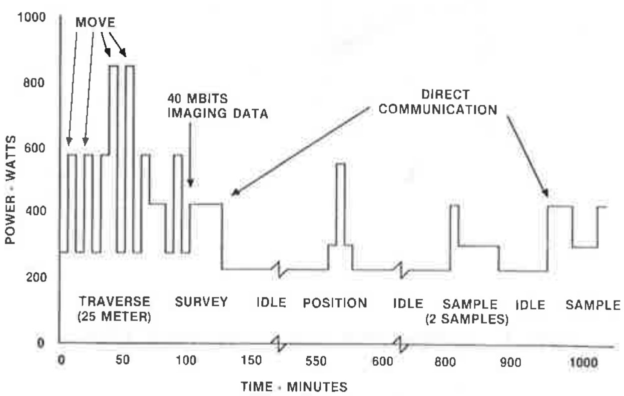

The number and location of RTGs on the Rover are very critical and require trade-off analysis. The Rover designers may prefer several small RTGs distributed around the vehicle, since this arrangement can help in the load distribution and facilitate the use of the RTGs' waste heat for thermal management of the Rover body and electronics bays. Also, shorter RTGs are less likely to block other Rover instruments and/or antennas. On the other hand, longer RTGs offer a higher specific power, because of decreased end losses and weights. They also are less likely to obscure the view of each other's radiators to space. At present, two concepts for integrating the RTGs with the Rover are undergoing evaluation, one employing two 250-watt RTGs, and one employing four 125-watt RTGs mounted on top of the Rover. The four-RTG option was illustrated in Figure 3, and the two-RTG option was shown in Figure 4. Either option could be used with either type of vehicle. Note that the RTGs are mounted vertically, to prevent build-up of sand on their heat rejection surfaces during Martian storms.

3.2 RTG ENVIRONMENT

Both the Rover and Mars environments present new challenges to the RTG designer. Previous RTGs (MHW, GPHS) were designed primarily for operation in microgravity and in a high vacuum after launch. The Rover and Mars environments are more difficult, mechanically, thermally, and atmospherically.

From the dynamic-environment point of view, the Rover RTG has to withstand launch, entry, landing, and traverse loads that occur at different times in the life of the mission. These loads cannot be accurately determined until the spacecraft and Rover structures are better defined. In the absence of such definition, the RTG design study was conservatively based on 3-axis design loads of 25 G during Earth launch, and 15 G during the Mars landing and for the balance of the four-year mission.

During entry into the Martian atmosphere, the Rover-mounted RTGs are enclosed in a protective aeroshell, as illustrated in Figure 6. While they are enclosed in that aeroshell, they are unable to radiate their waste heat to space, and will therefore require an auxiliary cooling loop. For short periods, during Earth launch and Mars entry, a water boiler dumping steam overboard could be used as the loop's heat sink. But for the much longer orbital transit period, a steady state-heat rejection system is required. Therefore, during the cruise to Mars, the RTGs will either require a mechanism for their temporary deployment outside the aeroshell, to permit radiative cooling; or will require continuous operation of the auxiliary cooling loop to transfer their waste heat to radiators located on or outside the Rover's aeroshell. The latter option is probably preferable, because it avoids the mechanical complexity and potential unreliability of a deployment mechanism. The necessary reliability of the auxiliary cooling loop can be achieved by the use of redundant cooling pumps.

Figure 6. Rover with RTGs and Lander Enclosed in Aeroshell

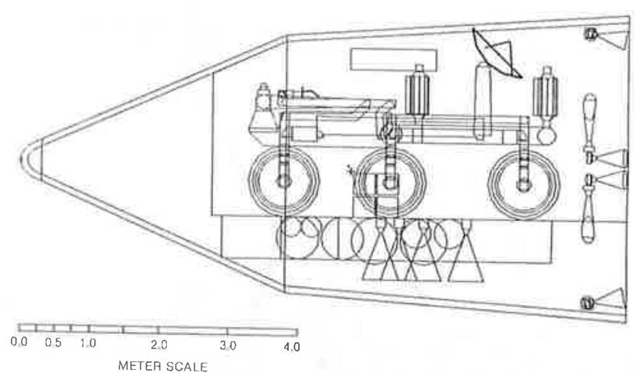

The most difficult problem imposed by the Mars surface environment is the presence of an external atmosphere [9]. The thermoelectric converter elements in the RTG are embedded in multifoil thermal insulation, to minimize heat losses from the hot heat source to the cool generator housing. Thus, the insulation forces most of the heat to flow through the thermoelectric legs. Multifoil insulation performs well in the absence of conducting gases, but degrades rapidly when such gases are present. Moreover, at the projected operating temperatures even small amounts of some of the Martian gases would react with the converter's materials and degrade its performance. Therefore, inleakage of Martian gases and buildup of alpha-generated helium in the converter must be prevented.

4.0 DESIGN APPROACH

The present paper first summarizes the design of a "baseline" RTG and its performance parameters. It then presents RTG designs and analytical results for a number of alternative design options, including more advanced (and less developed) converter configurations and thermoelectric materials.

The baseline design employs proven components and performance parameters. To minimize the need for new developments, it is conservatively based on: standard General Purpose Heat Source modules, which have been developed and safety-qualified for the Galileo mission; standard SiGe unicouples, developed and extensively lifetested for the Voyager and Galileo missions; and thermoelectric performance parameters and degradation rates that have been demonstrated in extended ground tests and space missions.

A more detailed description of the baseline RTG's design, mass breakdown, and of its structural, thermal, thermoelectric, and electrical analyses for a variety of environmental conditions is presented in a separate Fairchild report [1] available from the author.

4.1 HEAT SOURCE

DOE has spent approximately ten years and \$40-50M on the development [10] and safety qualification [11] of the General Purpose Heat Source (GPHS), for initial deployment on the Galileo and Ulysses space exploration missions. As a result of that effort, this heat source is extremely well characterized, much more so than radioisotope heat sources used on previous space missions.

Figure 7. General-Purpose Heat Source Module (250 Watt)
Sectioned At Midplane

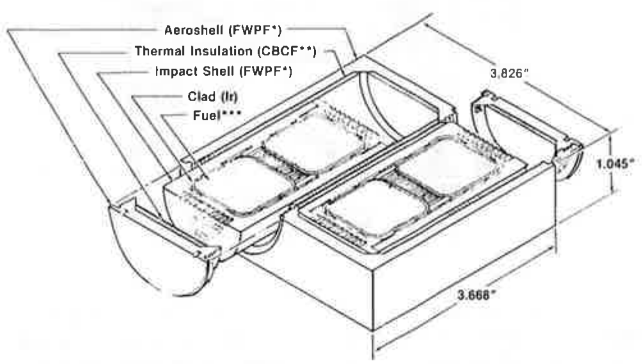

*Fine-Weave Pierced Fabric, a 90%-dense 3D carbon-carbon composite
**Carbon-Bonded Carbon Fibers, a 10% dense high-temperature insulator
***62.5-watt $^{238}PuO_2$ pellet

The heat source is modular, and a sectioned view of a standard 250-watt module is shown in Figure 7. Each GPHS module contains passive safety provisions against fuel release for all credible accident conditions. As shown, each module contains four iridium-clad $Pu^{238}O_2$ fuel capsules surrounded by graphitic components, including an aeroshell designed to withstand reentry ablation, a thermal insulator to avoid excessively high clad temperatures during the reentry heat pulse and excessively low clad temperatures at earth impact, and an impact shell to help absorb impact energy and reduce fuel capsule deformation during earth impact. Viewed from the outside, each GPHS module is a graphite brick of roughly 2 x 4 x 4 inches. This module was used as the building block for all RTG design options discussed in this paper.

4.2 THERMOELECTRIC UNICOUPLES

The baseline RTG design is based on standard SiGe unicouples and demonstrated thermoelectric performance levels and degradation rates. A very extensive experimental data base exists for such unicouples. Large assemblies of SiGe unicouples have operated successfully in the MHW RTGs flown on the Voyager and LES 8/9 mission and in the GPHS RTGs for the Galileo and Ulysses missions. They have demonstrated stable performance with moderate and predictable degradation rates for periods in excess of 100,000 hours, most recently on the Neptune flyby twelve years after launch of the Voyager.

The design of the standard unicouple is depicted in Figure 8. The p- and n-doped SiGe legs are 0.8" long, and the 1"-square hot-shoe collects the heat radiated by the heat source and delivers it to the TE legs. The cold end of the unicouple is bolted to the RTG housing, and the electrical connections between couples are made on the inside of the housing. There is no physical contact between the cantilevered unicouples and the heat source.

Figure 8. Unicouple

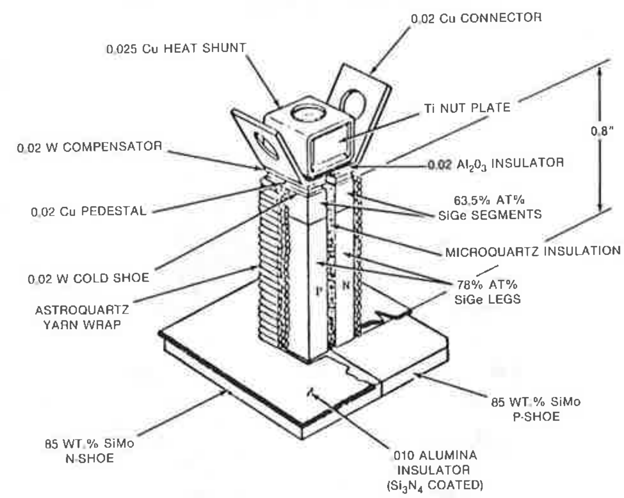

5.0 KEY DESIGN ISSUE

5.1 PROBLEM

The key problem in designing an RTG for Mars surface operations is the need to vent the helium generated by the fuel's alpha decay to the outside without allowing the Martian atmosphere to enter into and build up harmful quantities within the RTG. In the 1976 Viking mission to Mars, the 35-watt RTGs used fibrous insulation, which is much less effective than multifoil and leads to a substantially higher system mass. However, the more efficient and compact multifoil insulation used in the present study is only effective in a good vacuum (<1 torr). But the existing GPHS-RTG and Mod-RTG both use a large number of metal C-ring seals. Such seals are adequate for retaining the inert cover gas during the short launch period, but not for preventing intrusion of the Martian atmosphere during extended Mars operations.

To prevent helium pressure buildup inside the RTG above 1 torr, the use of a selective vent has been considered. But to maintain an internal helium pressure of less than one torr, such a vent would have to have a very low flow resistance. However, a low-flow-resistance vent would allow appreciable back diffusion of Martian gases into the RTG. This would be unacceptable unless these Martian gases were effectively gettered as soon as they entered the RTG. Even small quantities of Martian gases (CO, CO_2, O_2) would result in deleterious reactions with the RTG materials.

5.2 PROPOSED SOLUTION

Since the system of selective vent and effective getter has not yet been demonstrated, the Fairchild study was based on RTG designs with an evacuated annular converter, sealed off from the both the internal helium and the external Mars atmosphere.

This is illustrated in Figure 9a, which shows a horizontal cut through the active region of the baseline RTG; i.e., through the midplane of a heat source module and through the midplane of a ring of thermoelectric unicouples. Different shading patterns are used to designate the helium volume inside the heat source canister and the Martian atmosphere outside the RTG housing. As shown, the intervening annular converter is evacuated, and is separated from the helium by the heat source canister and from the Martian atmosphere by the RTG housing.

Figure 9a. Horizontal Cut Through Baseline RTG

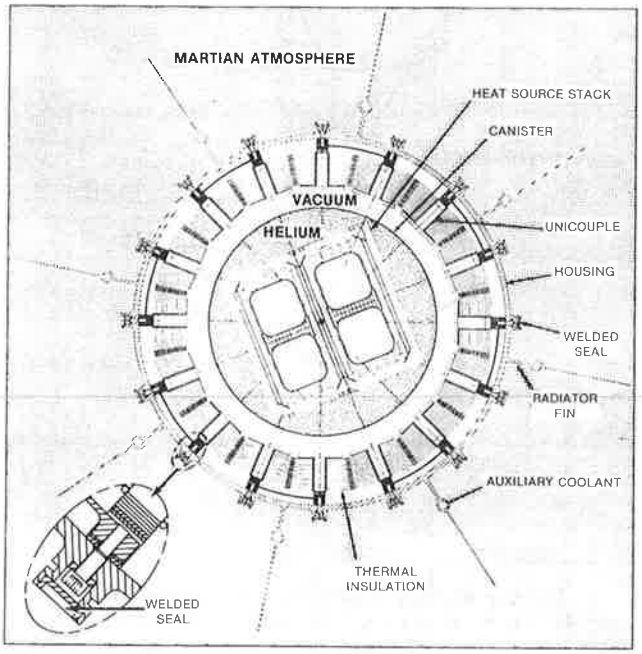

6.1 DESIGN DESCRIPTION

Figure 9b shows a cutaway view of the top of the thermoelectric converter, before insertion of the radioisotope heat source. The converter contains 576 SiGe unicouples. These are arranged in 36 horizontal rings, each consisting of 16 equispaced unicouples, depicted earlier in Figure 8. Each unicouple has a ~1"x1" heat collector, which concentrates the heat radiated from the heat source and delivers it to the couple's n- and p-legs. Heat transfer from the heat source canister to the unicouples is by radiation across a vacuum gap, without any physical contact. The RTG design is based on a maximum hot-junction temperature of 1000°C, which is the temperature at which unicouple assemblies have demonstrated long-term reliability and performance stability in extended ground tests and space operations.

As indicated in Figure 9b the 576 thermoelectric couples are embedded in 0.8"-thick thermal insulation, to minimize heat loss to the cooler RTG housing. The insulation consists of 60 layers of 0.0003" molybdenum foils separated from each other by alternating layers of quartz cloth. This is a very conservative insulation design, whose reliability has been demonstrated in long-term ground tests and space operations. The alternative of separating the molybdenum foils with zirconia particles instead of quartz cloth, which has been successfully used in more recent thermoelectric converter assemblies, would lead to considerably lighter and more compact insulation packages.

Figure 9b. Unfueled Converter

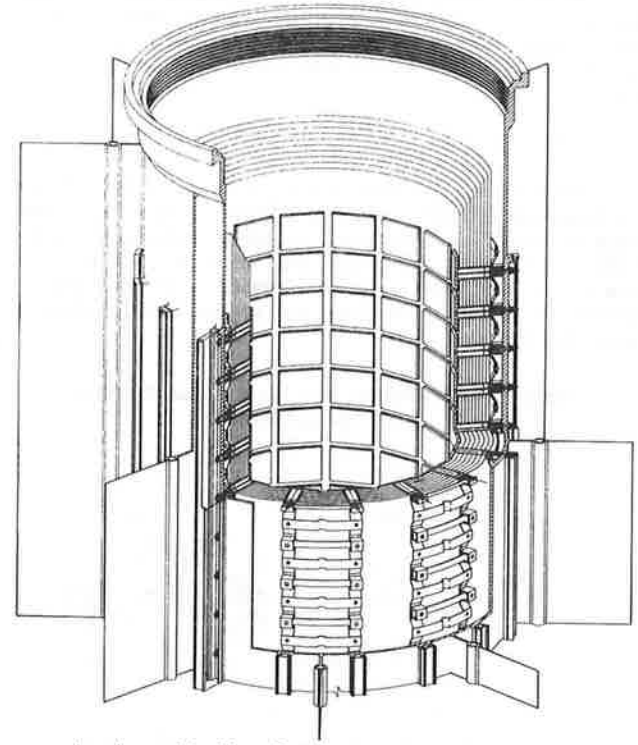

At the cold side of the thermal insulation, the 576 unicouples are connected in a series-parallel network. Couples are connected in parallel groups, to eliminate the risk of single-point failures. If any couple were to experience open-circuit failure, its partner(s) would carry the increased current, permitting continued RTG operation. There are 144 parallel couple groups in series, to build up the desired RTG output of 30 volts. To avoid the risk of shorts-to-ground causing single-point failures, the circuit is not grounded to the RTG housing.

The cold ends of the 576 unicouples are bolted to the RTG's 0.090"-thick aluminum housing. In the Galileo RTG, the unicouple bolt holes were sealed by metal c-rings, but these would be inadequate for preventing inflow of the Martian atmosphere during the four-year mission. As shown in the enlarged inset at the lower left corner of Figure 9a, the bolt holes in the present design are sealed by 16 aluminum cover strips welded to the aluminum housing ribs.

The unicouples deliver their waste heat to the RTG's aluminum housing. The housing and its eight fins serve to reject the RTG's waste heat, either by radiation to space or (when direct radiative cooling is not possible) by convection to the auxiliary coolant in the fins' integral cooling tubes.

Figure 10 shows a partially exploded cutaway view of the top of the RTG, after fueling. At its center is the heat source, consisting of a stack of 18 GPHS modules. The heat source stack is contained in a cylindrical molybdenum canister which acts as a helium container. The canister's end caps serve to provide the lateral support and axial compressive load to the ends of the heat source stack. The stack does not touch the canister along its length, and does not have any midspan supports.

The conservative baseline RTG, designed to produce 250 watts(e) at the end of the 4-year MRSR mission (i.e., 7 years after fuel encapsulation), has an overall height of 45.9 inches, a housing diameter 9.1 inches, and a tip-to-tip span of 15.2 inches.

Figure 10. Baseline RTG, Upper End

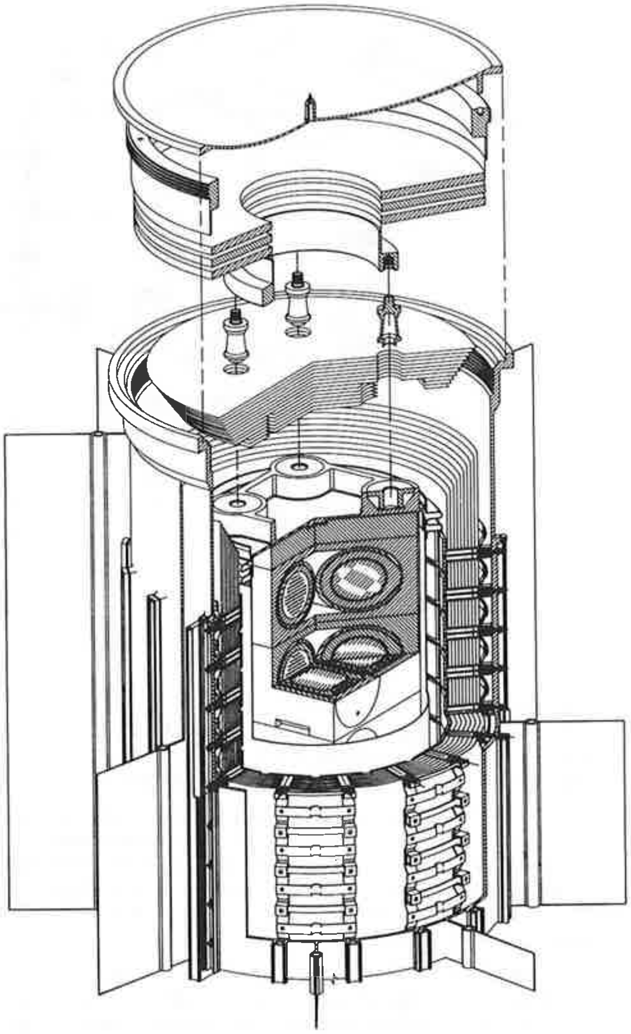

6.2 HEAT SOURCE SUPPORT

One of the most critical issues in designing an RTG with stacked heat source modules is the scheme for supporting that stack.

The GPHS module design is primarily driven by safety considerations. The modules are designed to survive hypersonic reentry and subsequent ground impact without fuel release. To maximize the impact safety margin, one wishes to minimize the impact velocity. Individual modules have a much lower impact velocity (49 m/s) than the stacked heat source (74 m/s). Therefore, it is desirable to support the heat source stack in such a manner that the individual modules separate in case of inadvertent reentry into the Earth's atmosphere. Automatic separation is accomplished by structurally supporting the heat source stack from the RTG's aluminum housing, which melts during reentry, releasing the modules. But the same support structure must hold the stacked modules together during launch and operational vibration and shock loads.

6.2.1 Description of Support Structure: The heat source support arrangement will be described in detail with respect to the baseline RTG design, and the same basic arrangement is used in the alternative RTG designs discussed in the companion paper [1]. Since the heat source stack is only supported at its ends and there are no midspan supports, a large (5500-lb) axial preload is required to hold the stack together during launch under the assumed 25-G transverse load. The axial preload is applied directly to the ends of the stack, via the canister's end caps. The canister's side wall plays no structural role; it is merely a helium container, and is thin enough to burn off during reentry.

Figure 11 presents an exploded closeup of the support structure at the top of the heat source stack. As shown, the top of the heat source stack is followed by a graphite transition section which bears against the top cap of the molybdenum canister via a thin iridium sheet that serves as a reaction barrier between the graphite and the molybdenum.

On the outside of the canister end cap is a set of integral stiffening ribs and load stud seats. These form a square structure, to spread the axial load from the four load studs to the four edges of the heat source end face. The four studs at each end are similar to those used in the Galileo RTG. They are made of low-conductivity Inconel, and are separated from the stud seats by zirconia insulators to reduce axial heat losses and to lower the temperatures of the creep-prone Inconel studs and titanium springs. As indicated in Figure 11, the load studs penetrate through the multifoil thermal insulation.

Figure 11. Support Structure at Top of Heat Source

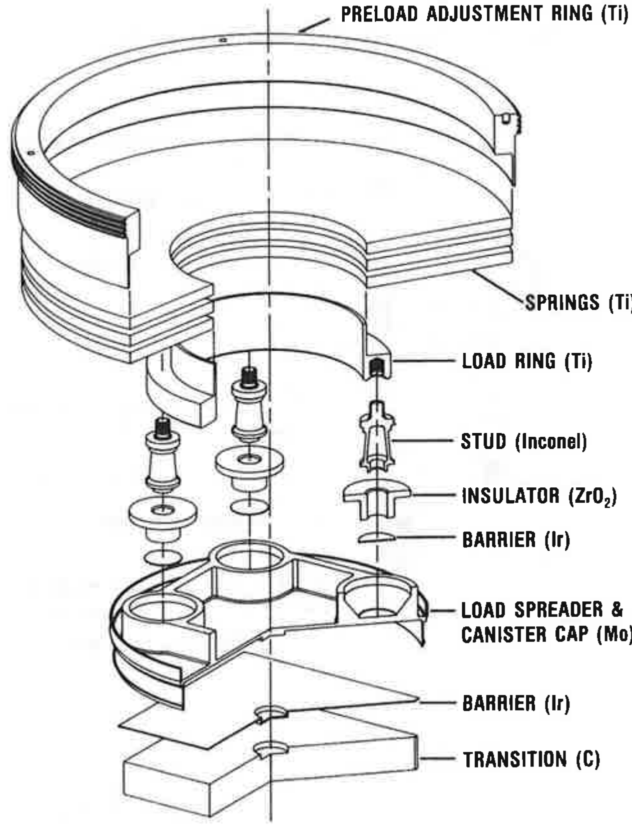

The tops of the four studs are bolted to a titanium load ring, which is laterally supported and axially loaded by a set of three nested Belleville springs made of 0.2"-thick titanium. Three springs are used in order to generate the required preload without exceeding the allowable stress in the springs. The I.D. of the bottom spring bears against the load ring, and the O.D. of the top spring bears against a titanium preload adjustment ring that is threaded to the I.D. of the aluminum housing. After the load is set, rotation of that ring is prevented by pins protruding from the RTG's aluminum cover. That cover serves only as a pressure dome, and has no other structural function.

Clearly, the heat source stack is ultimately held together by the RTG's low-melting aluminum housing. When that housing and the thin canister burns away during reentry, the heat source modules are free to disperse and impact individually.

Figure 13 shows an exploded view of the heat source's lower support structure (viewed from below), and Figure 14 shows a cutaway view of the lower end of the assembled RTG. As can be seen, the lower support structure uses an identical set of load spreaders, zirconia insulators and Inconel studs as the upper support structure. But there are no springs, and the studs are mounted directly on the RTG's aluminum base plate. The base plate employs 1" x 0.25" radial and circumferential ribs to provide the required stiffness.

The figures also show the helium vent tube at the center of the canister's base. The vent tube passes through the evacuated converter region and is sealed to the RTG base plate. A bimetallic joint is used to seal the vent tube to the aluminum base plate. Similar bimetallic joints are used to connect the aluminum base plate to the metal-ceramic seals which serve for the electrical isolation of the RTG terminals.

Figure 12. Support Structure at Bottom of Heat Source

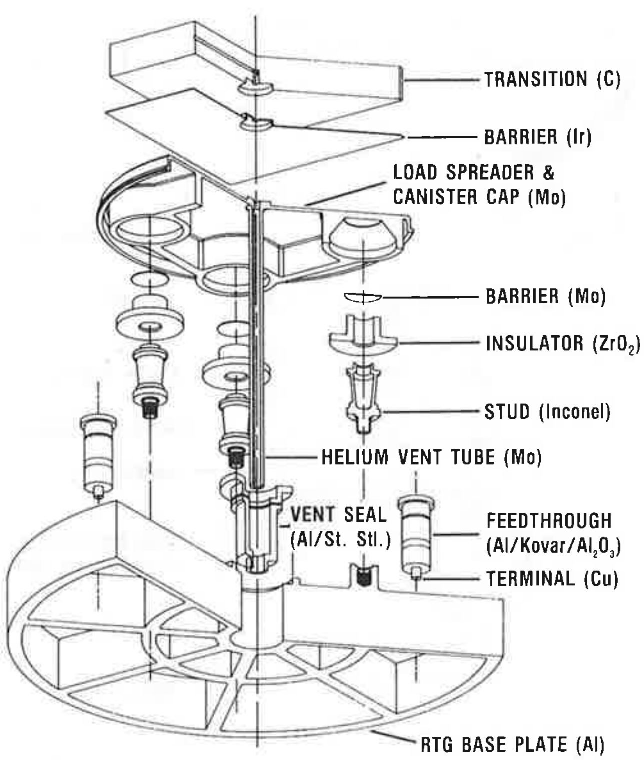

Figure 13. Lower End of Assembled RTG

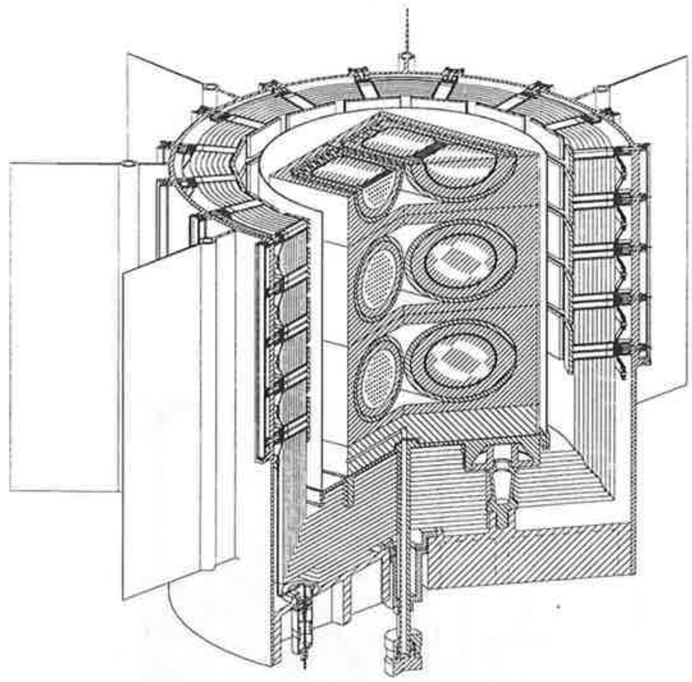

The helium generated by the fuel's alpha decay is vented to space, through a semi-permeable Viton seal which prevents inflow of the Martian atmosphere into the heat source canister. In effect, the Viton seal acts as a pressure relief device.

The Belleville springs shown in Figures 11 and 12 must supply sufficient force to enable the heat source stack to withstand the lateral G-loads during launch while the RTG fins are water-cooled. Once the Rover aeroshell is discarded after entry into the Martian atmosphere, the RTG is cooled radiatively for the balance of the mission.

When changing from water-cooling to radiation cooling, the RTG housing temperature rises about 100°C (on a summer day). This causes a differential growth of about 0.100" in the length of the high-expansion aluminum housing relative to the low-expansion graphite heat source stack, with a corresponding increase in the Belleville spring length and drop in spring force. In RTGs for other missions, the magnitude of the spring force is only important briefly during launch. In the case of the Rover RTG, the springs must still provide sufficient force after relaxation to hold the heat source together during Mars traverses for the balance of the four-year mission.

The structural analysis and design of the RTG consists of three principal tasks:

1. Determining how large a preload is required to hold the modules together during Earth launch and during Mars operations.
2. Designing the Belleville springs to supply the required spring force and spring travel.
3. Determining the stresses in the heat source modules, and designing the RTG housing to withstand the bending moments on the cantilevered RTG during launch, to be structurally stable against the one-atmosphere external pressure on earth, and to stay below the stresses where long-term creep would occur at the materials' operating temperatures.

6.2.2 Required Heat Source Preload Force: The heat source stack may be viewed as a partitioned beam with a distributed side load. If the beam were continuous rather than partitioned, the side load would produce axial compressive stresses on the side to which it is applied, and axial tensile stresses on the opposite side. But a partitioned beam cannot sustain a tensile stress in the axial direction. Therefore, in the absence of an axial preload, the side load would cause the partitioned beam to fall apart. To hold the heat source stack together in the RTG, the axial preload must be high enough to equal or exceed the maximum axial tensile stress produced by the side load.

To assess the magnitude of the required axial load, a detailed solids model of the GPHS module's aeroshell was constructed, and a stack of 16 such modules was subjected to a side load of 25 G and an axial load of 4000 lbs (17,800 Newton). In the initial NASTRAN analysis, the heat source stack was analyzed without the effect of the simultaneous deformation of the cantilevered RTG housing. This simplification cuts the problem in half, because it results in identical end supports and symmetry about the heat source's midplane. The resultant deformation of the upper half of the 16-module stack is shown in Figure 14.

Figure 14. Deformation of Upper Half of Heat Source Stack Under 4000-lb Axial Load and 25G Side Load (Y)

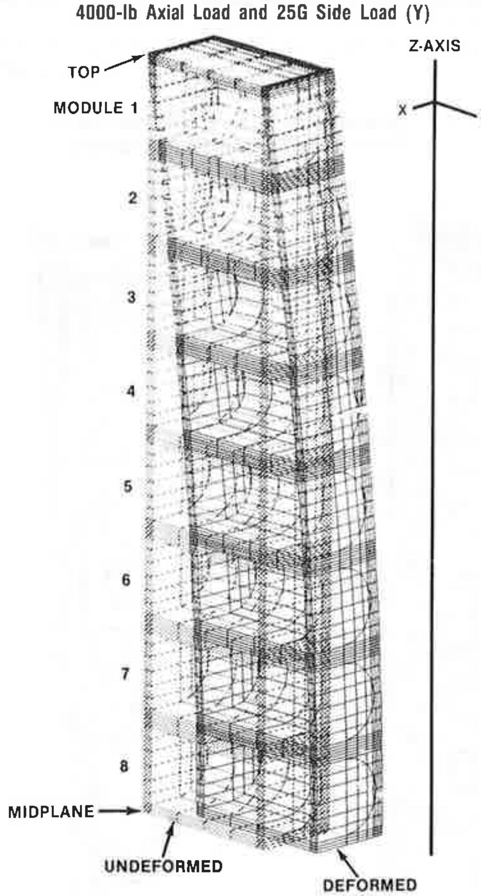

The corresponding distribution of heat source stresses was analyzed, using orthotropic properties for the carbon-carbon composite (FWPF). All normal-Z stresses were found to be negative (i.e., compressive), except in Module 1 where one small corner section was found to exhibit a tensile stress of 0.53 ksi (3.7 MPa), as shown in Figure 16. It was therefore concluded that the 4000-lb preload is slightly inadequate for the 16-module heat source. Based on these results, it was decided to use a 5500-lb preload for the 18-module heat source in subsequent analyses.

Figure 15. Normal Z-Stresses in Top GPHS Module (in ksi) (1 ksi=6.89 MPa)

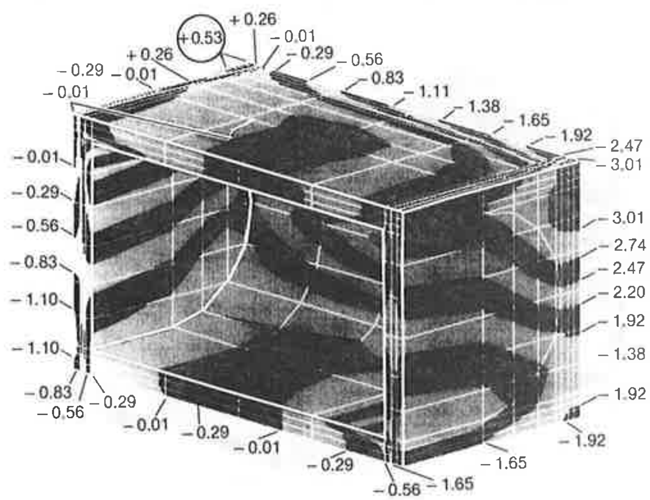

6.2.3 Designing the Belleville Springs: The Mars Rover RTG design differs from other RTGs in that a preload is required not just for a brief period during Earth launch, but also during atmospheric entry and landing on Mars and during Rover activities on Mars for the full four-year duration of the MRSR mission. Although the G-loads during these post-launch operations (15 G) are lower than during launch (25 G), one cannot assume that springs which satisfy the higher requirement will automatically satisfy the lower. This is so because the Rover RTG is water-cooled during Earth launch and radiation-cooled during and after Mars landing, as previously explained.

In switching from water-cooling to radiation-cooling, the RTG's housing temperature rises by about 100°C, causing its length to grow by about 0.1″. Since the thermal expansion of the graphite heat source is virtually negligible, the thermal growth of the aluminum housing causes a corresponding expansion of the Belleville preload springs, and consequently a relaxation of the compressive load on the heat source stack.

Therefore, the designer must consider the adequacy of the spring force both during launch and during subsequent Martian operations, at their respective RTG temperatures. At the same time, he must make certain that the maximum stress in the spring material under maximum-load conditions does not exceed the spring material's strength at temperature. Thus, the spring design must satisfy three independent constraints.

As shown in the full report [1], satisfying those three constraints requires the solution of simultaneous cubic equations. The spring design was for an outer diameter of 8.75 inches, to mate with the inside of the RTG housing, and an inner diameter of 3.20 inches, to mate with the load ring. The springs were designed to deliver an axial load of 5500 lbs in the water-cooled RTG and 3300 lbs in the radiation-cooled RTG. The titanium spring alloy was assumed to have an elastic modulus of 11 x 10^6 psi, a Poisson ratio of 0.31, and an allowable compressive stress of 82 ksi. For these parameters, it was found that the three design goals could be satisfied with a single set of three nested springs, each having a thickness of 0.221 inch, a free height of 0.451 inch, and a compressed height of 0.275 inch in the water-cooled RTG and 0.375 inch in the radiation-cooled RTG.

6.2.4 Von-Mises and Shear Stresses in Heat Source: The same solids model depicted in Figure 14 was used to compute the von Mises stresses in the modules. The maximum stresses were found to occur in Module 1, and are shown in Figure 16.

Figure 16. Von Mises Stresses in Module-1 (in ksi)

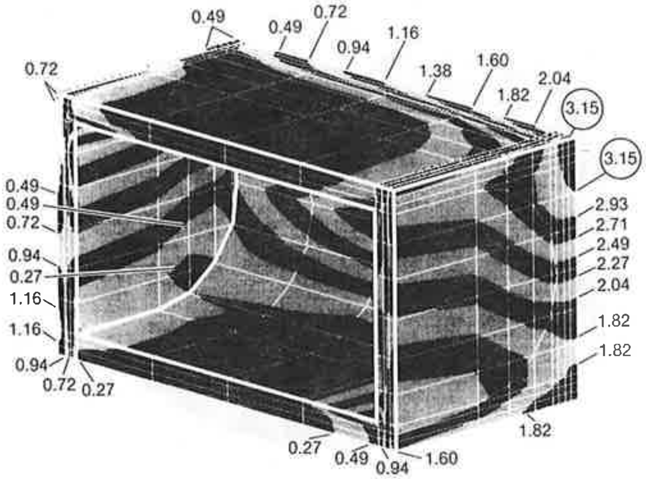

As can be seen, the maximum von Mises stress, in the upper right corner of Module #1, is 3.15 ksi. This is only 15% of the tensile and compressive strengths of the Fine-Weave Pierced Fabric (FWPF) graphite material, as shown in Table 1, which was supplied by its manufacturer AVCO.

Table 1. Composite Strength (ksi) of AVCO Fine-Weave Pierced Fabric

TEMPERATURE:	°F	75	600	1000	2000	3000	4000	5000
	°C	24	316	537	1093	1649	2204	2760
TENSION:	Y	17.74	19.66	20.66	23.86	26.21	27.39	25.20
	X	17.64	19.66	20.66	23.86	26.21	27.38	25.20
	Z	18.17	20.24	21.28	24.57	26.99	28.20	25.95
COMPRESSION:	Y	20.61	20.78	20.85	21.59	23.56	26.49	30.61
	X	20.61	20.78	20.85	21.59	23.56	26.49	30.61
	Z	20.8	21.0	21.11	21.89	23.89	26.66	31.00
SHEAR:	YZ	1.17	1.11	1.07	1.00	0.99	1.26	1.00
	ZX	1.17	1.11	1.07	1.00	0.99	1.26	1.00
	XY	1.17	1.11	1.07	1.00	0.99	1.26	1.00

Figure 17. Module-1 YZ-Shear Stresses, in ksi

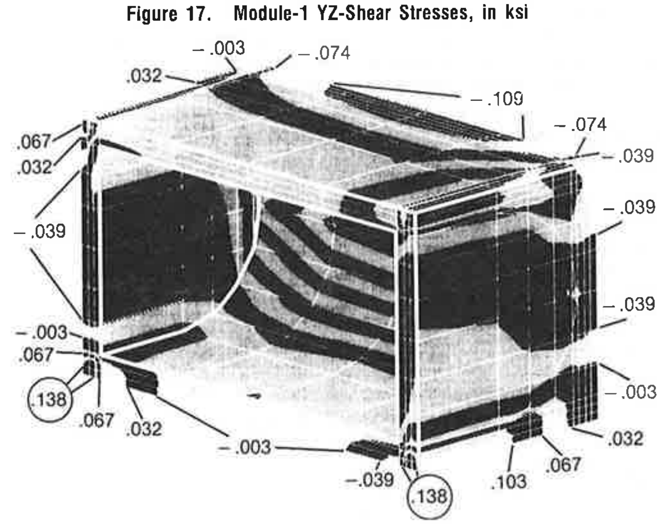

Table 1 shows that FWPF is much weaker in shear than in tension or compression. Therefore, the xy, xz, and yz shear stresses were computed. The maximum shear stress was found to be the yz-stress in Module 1. As shown in Figure 17, the maximum shear stress is 0.138 ksi. This is only 14% of the material's shear strength shown in Table 1.

6.2.5 Deformation and Stresses in Full RTG: The preliminary structural analysis described thus far employed a simplified analytical model that did not include the RTG housing, which supports the load springs that compress the heat source stack. In the more complete analysis described in the full report [1], the heat source was supported by the deformable RTG housing. Specifically, the upper springs were connected to the top of the housing side wall, and the lower heat source support studs were mounted on the housing baseplate.

The model of the housing included the fin roots and cooling ducts which act as stiffeners. It also included the radial and circumferential stiffeners of the baseplate. The housing was cantilevered, with only the rim of its baseplate fixed and the rest of the housing free to lean away from the 25-G side load. The resultant angular deflection of the RTG's upper end resulted in highly unsymmetrical heat source supports. Therefore, it was necessary to model the whole 18-module heat source.

The solids model used for the preliminary analysis of the eight-module half-stack had 10,961 grid points and 26,652 degrees of freedom. Using a similar solids model for the full eighteen-module heat source would have exceeded the available

Figure 18. Deformation of Spring-Loaded Heat Source Supported by Cantilevered RTG Housing

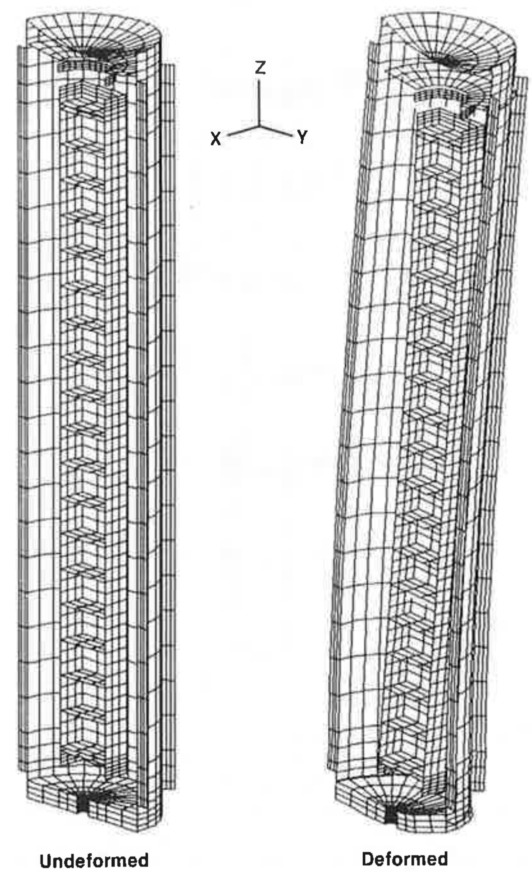

computer time and disk space. To avoid that, the solids model was replaced with a plate model having an equivalent stiffness matrix. Even so, a very large (2140-node) NASTRAN model with 10,611 degrees of freedom was required to represent the heat source, its support structure, and the RTG housing.

Figure 18 depicts the model of the RTG in its undeformed and deformed shapes. The deformation shown includes the effects of the 25-G side load and of the 5500-lb spring force, which produces a compressive load on the heat source stack and a tensile load on the housing.

The deformations shown have, of course, been exaggerated for improved visibility. Note the leaning of the housing and the bowing of the heat source in the y-direction, the axial elongation of the housing due to its tensile load, and the outbowing of the RTG's baseplate due to the downward force exerted by the heat source.

Figure 19. Stresses in Heat Source Aeroshells (ksi)

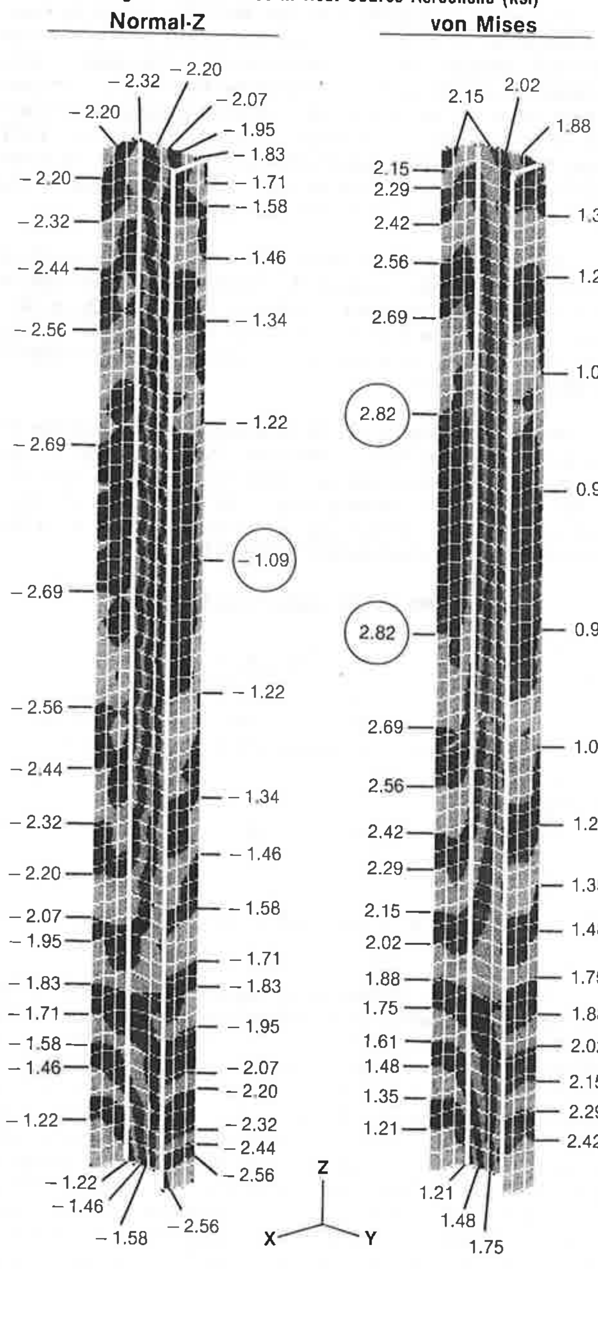

Figure 19 presents the normal-Z stresses and von Mises stresses in the heat source side walls. As can be seen, all of the normal-Z stresses are negative. The highest (i.e., least negative) Z-stress is -1.09 ksi, well within the compressive regime. The computed results suggest that the 5500-lb preload can probably be reduced to 5000 lbs without developing any tensile Z-stresses.

The right half of the figure shows that the maximum von Mises stress, 2.9 ksi, is again far below the strength limit of the FWPF graphite material. (See Table 1.)

The corresponding von Mises stresses in the side wall of the RTG housing are depicted in Figure 20. Two conditions are illustrated: The left half of the figure shows the short-term launch stresses of the water-cooled RTG housing with a 5500 lb spring load and a 25 G side load. The right half of the figure shows the long-term stresses of the radiation-cooled RTG with a 3300 lb spring load and a 15 G side load.

Figure 20. Von Mises Stresses in Housing Side Wall (ksi)

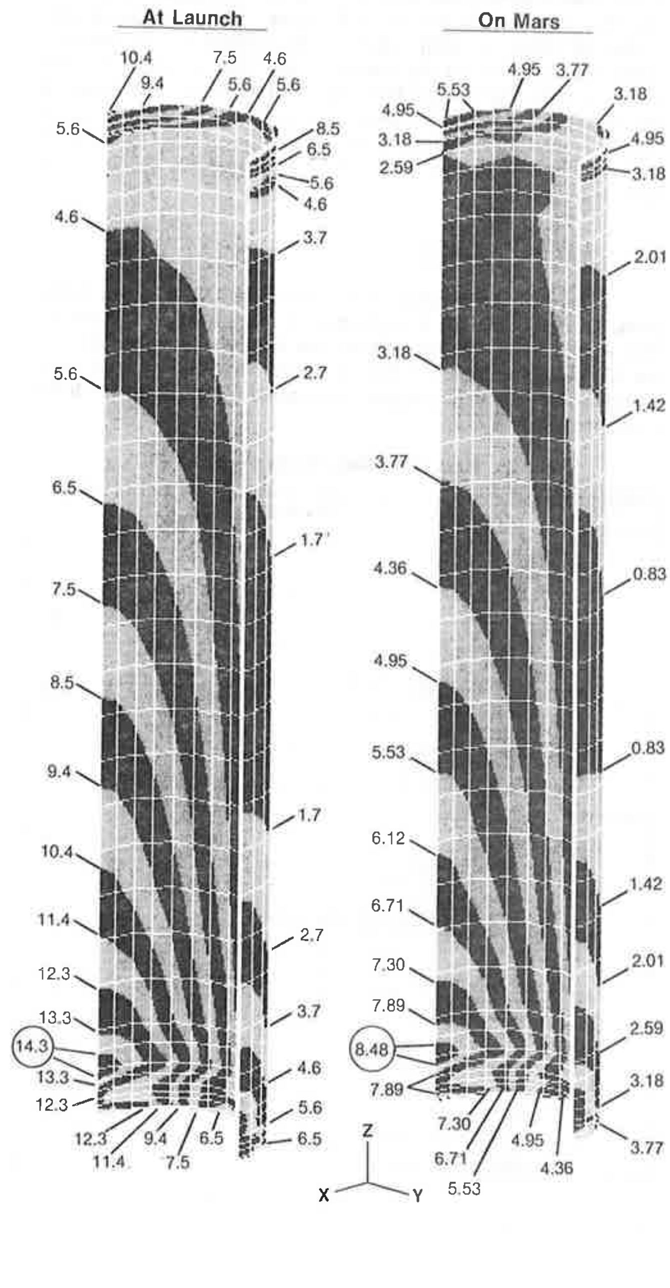

The maximum launch stress, which occurs at the -y side near the base of the RTG, is ~15 ksi. This is well below the 31-ksi yield strength of the aluminum alloy (2219 T851) at its 171°C launch temperature. Similarly, the maximum stress on Mars, 8.5 ksi, is only 53% of the alloy's 16-ksi yield strength at its 272°C maximum operating temperature.

In addition to yield strength, the long-term creep characteristics of the aluminum housing must be considered. The RTG housing, at its thinnest (0.090") section, has a horizontal cross-section of 2.54 in^2. Thus, at its maximum operating temperature, the 3300-lb spring load will produce a steady-state tensile stress of 1.3 ksi. Even if the housing were constantly at its maximum Martian operating temperature of 272°C, this tensile stress would produce only negligible creep during the four-year mission.

The same structural-analysis model was used to determine the stresses in the RTG's 0.062"-thick top cap and in its 0.125"-thick base plate with 1" x 0.25" stiffening ribs. All stresses were found to be well below the strength of the aluminum alloy at temperature. In summary, the detailed NASTRAN analysis of the spring-loaded heat source supported by the cantilevered RTG housing confirmed the feasibility of supporting an 18-module heat source stack without midspan supports, and demonstrated the adequacy of the spring and housing dimensions on which the mass analyses in the next section are based.

6.3 MASS BREAKDOWN

The mass breakdown of the "baseline" Mars Rover RTG, depicted in Figure 10, is presented in the left half of Table 2. The right half of the table shows the corresponding breakdown for the existing Galileo RTG, to ensure that all required RTG components have been properly accounted for in the Rover RTG mass breakdown.

Table 2. Mass of Baseline RTG Versus Galileo RTG

RTG MASS BREAKDOWN (kg)	ROVER RTG BASELINE DESIGN		GALILEO RTG	
HEAT SOURCE (33.8/30.1kg)				
GPHS MODULES (18/18)		26.05		26.05
FUEL (PuO2)	10.73		10.73	
CAPSULES (Ir)	4.21		4.21	
GRAPHITICS	11.11		11.11	
H.S. CANISTER (Mo)		3.77		0.00
SIDE WALLS	2.21		----	
BELLOWS	0.11		----	
END CAPS AND LOAD SPREADERS	1.45		----	
H.S.STRUCTURAL SUPPORTS		3.94		4.05
GRAPHITE PRESSURE PLATES	0.52		0.53	
LOAD STUDS+ZIRCONIA	0.27		0.38	
BELLEVILLE SPRINGS (Ti)	2.31		0.51	
OTHER PRELOAD HARDWARE	0.84		1.69	
MID-SPAN SUPPORT ASSEMBLY	----		0.94	
CONVERTER (24.9/26.0kg)				
ELECTRICAL CIRCUITS		7.74		7.65
TE ELEMENTS (576/572)	5.43		5.40	
TE FASTENERS AND SEALS	1.09		1.08	
ALUMINA INSULATORS	0.88		0.88	
ELECTR. CONNECTORS +TERMINALS	0.34		0.29	
MULTIFOIL INSULATION (Mo/Quartz)		5.94		7.16
SIDES	5.26		5.52	
ENDS	0.68		0.55	
SUPPORT STRUCTURE	----		1.09	
RTG HOUSING (Al)		8.45		8.17
SIDE WALL (0.090"/0.060")	7.01		6.47	
COVERS & BOLTS	0.98		0.81	
RESISTANCE THERMOMETER	0.30		0.30	
GAS MGMT. ASSEMBLY	0.16		0.16	
PRESSURE RELEASE DEVICE	----		0.43	
RADIATOR		2.78		3.00
FINS (8/8)	2.38		1.96	
AUXILIARY COOLANT MANIFOLDS	0.25		0.26	
EMISSIVITY COATING	0.15		0.15	
MISCELLANEOUS ELEMENTS	----		0.63	
TOTAL RTG MASS (kg)		58.67		56.08

The left column of Table 2 shows that the baseline RTG has a total mass of 58.7 kg. As shown, most (58%) of that mass is in the heat source rather than the converter, and most of that (77%) resides in the heat source modules. It is also noteworthy that the heat source canister, which enables operation of the RTG in the Martian atmosphere, has a mass of 3.8 kg.

The right half of Table 2 shows the corresponding mass breakdown for the existing Galileo RTGs. As seen, the baseline Rover RTG, with its non-optimized radiator fins, is 4.6% heavier than the Galileo RTG. Most of that difference (3.77 kg) is due to the canister needed for Mars operations. The other subsystems have very similar masses in the two RTGs.

7.0 THERMAL AND ELECTRICAL ANALYSIS

The analysis described in this section consists of three parts (thermal, thermoelectric, and electrical), which must be performed simultaneously and interactively. The analysis uses specialized computer codes generated by Fairchild to compute the heat flows, temperatures, and electrical parameters of each layer of thermoelectric elements. Inputs include the RTG design, the thermal input power (BOM/EOM), the cooling mode (water/radiation, Mars environment), the TE materials and performance, and the desired electrical output voltage.

The required analysis cannot be carried out by a standard thermal analysis code, because the thermoelectric unicouple is not a simple heat conductor. The heat input rate Q_h at the couple's hot junction does not equal the heat rejection rate Q_c at its cold junction, since part of the input energy is converted into electrical power P.

As shown in Figure 21, the heat input rate Q_h consists of four terms: normal heat conduction, Peltier cooling, ohmic heating, and Thomson effect. The heat rejection rate Q_c consists of four corresponding terms. All but the first of those terms are functions of the couple current I, which must be derived from an analysis of the RTG.

Figure 21. Unicouple Energy Balance

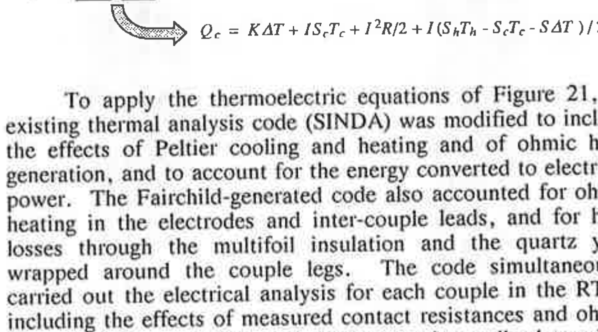

$$K = [k_n A_n + k_p A_p] / L$$

$$R = [\rho_n / A_n + \rho_p / A_p] L$$

$$Q_h = K\Delta T + IS_h T_h - I^2 R/2 - I(S_h T_h - S_c T_c - S\Delta T)/2$$

$$P = IV = I(S\Delta T - IR)$$

$$Q_c = K\Delta T + IS_c T_c + I^2 R/2 + I(S_h T_h - S_c T_c - S\Delta T)/2$$

To apply the thermoelectric equations of Figure 21, an existing thermal analysis code (SINDA) was modified to include the effects of Peltier cooling and heating and of ohmic heat generation, and to account for the energy converted to electrical power. The Fairchild-generated code also accounted for ohmic heating in the electrodes and inter-couple leads, and for heat losses through the multifoil insulation and the quartz yarn wrapped around the couple legs. The code simultaneously carried out the electrical analysis for each couple in the RTG, including the effects of measured contact resistances and ohmic losses in legs, electrodes, and leads; experimentally determined effects of long-term material degradation of SiGe; and optimized n/p leg area ratios. Other constraints applied were that all TE elements grouped in parallel must operate at the same voltage, and all groups in series must have the same current.

The analysis used temperature-dependent values of the Seebeck coefficient, electrical resistivity, and thermal conductivity for the SiGe n- and p-legs. Temperature-averaged properties were computed for each unicouple layer for each iteration of the analysis. They yielded a final value for the SiGe unicouple's temperature-averaged figure of merit [14] of 0.000583 K^{-1} at BOM and 0.000548 K^{-1} at EOM at the center of the baseline RTG. The thermal and electrical results were used to compute the material efficiency, couple efficiency, and converter efficiency of each layer of TE elements, and the overall RTG system efficiency.

The Fairchild-generated code was used to carry out the coupled thermal, thermoelectrical, and electrical analyses of the RTGs. A 425-node model of the axisymmetric RTG was used to compute the axial variation of the temperatures of the various RTG components. That axial variation is appreciable, because of unavoidable end losses through the structural supports at the top and bottom of the heat source stack. Each heat source module and thermoelectric element layer was discretely represented in the analysis

Figure 22 depicts the flow chart of the Fairchild's Thermal-Thermoelectric-Electrical Analysis code (TTEEA). As can be seen, it consists of three nested loops. The analysis starts with initial guesses for the RTG's temperatures T_o, current I_o, and couple area A_o. The thermoelectric subroutine then computes the temperature-averaged thermoelectric properties and the heat input Q_h and output Q_c of each layer of couples in the RTG. These values are fed into the thermal analysis subroutine, which calculates a new set of RTG temperatures. This inner loop is repeated until the temperatures have converged.

Figure 22. Thermal-Thermoelectric-Electrical Analysis Code (TTEEA)

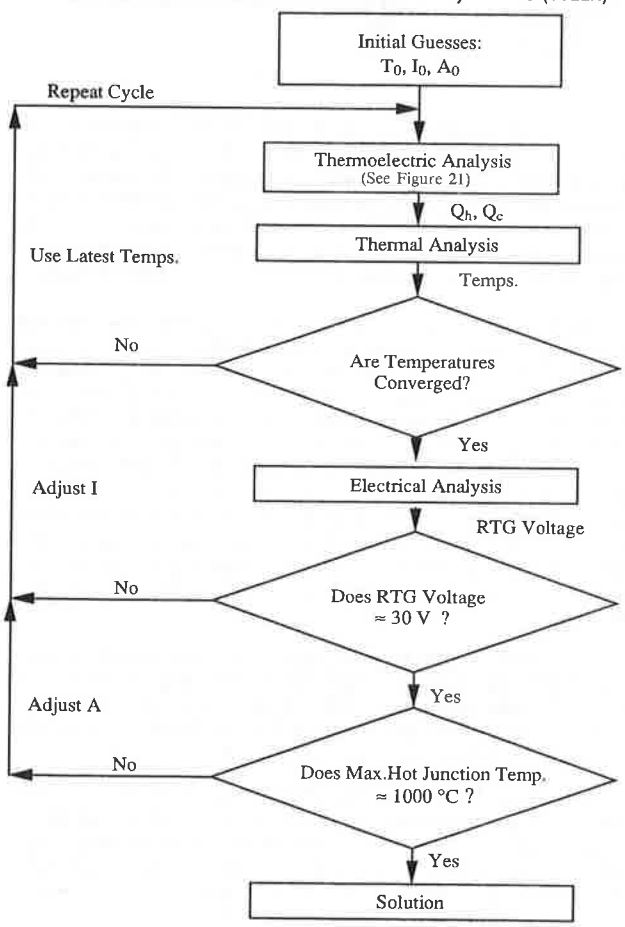

Next, the electrical analysis subroutine is used to compute the voltage of each couple and the output voltage **V** of the whole RTG. If it has not converged to the desired 30-volt output, the middle loop is repeated with adjusted values of the current **I** until convergence is achieved.

The code then searches for the maximum hot-junction temperature T_{max} and repeats the outer loop with adjusted values of the couple area **A** until T_{max} converges to the BOM design goal of 1000°C. For subsequent EOM analyses, the outer loop is omitted since the leg area **A** has already been fixed by the BOM anlysis.

7.1 TEMPERATURE DISTRIBUTION

Figure 23 shows the beginning-of-mission temperature distribution (in °C) of the radiation-cooled baseline RTG for a 300°K sink temperature. It shows the temperatures of the RTG end regions, and the temperatures at the center of the RTG. The temperatures shown are for an RTG with unicouples of standard dimensions, except that the cross-sectional areas of their SiGe legs have been reduced by 9% from the corresponding values in the Galileo RTG. This was done in order to take full advantage of the unicouples' maximum temperature capability.

Figure 23. BOM Temperature Distribution (°C) in Baseline RTG

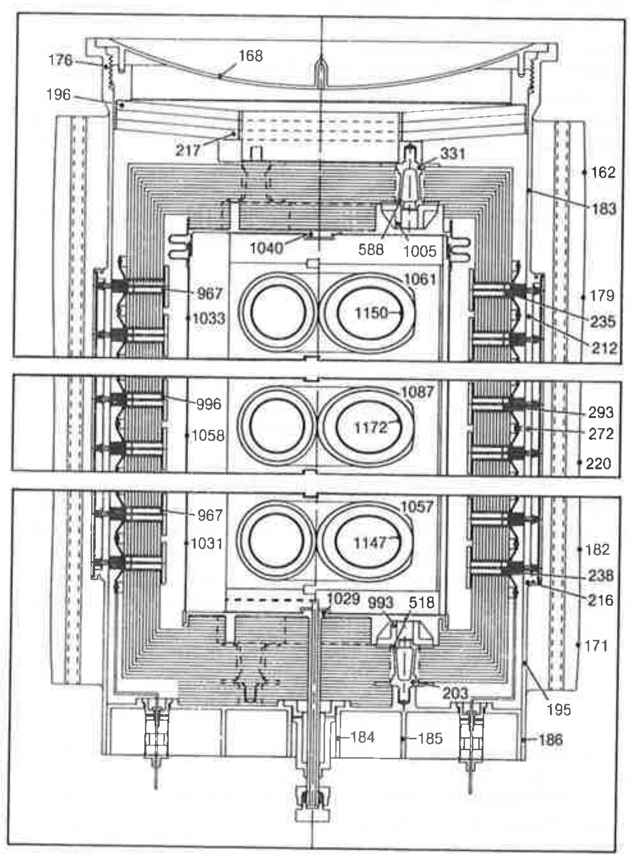

The figure shows the maximum temperatures of the iridium capsules (1172°C), the graphite heat source surface (1087°C), the molybdenum canister (1058°C), the SiGe hot junction (996°C) and cold junction (293°C). Of particular interest are the maximum temperatures of the zirconia insulators (1005°C), the Inconel support studs (588°C), the titanium springs (217°C), and the aluminum housing (272°C), since their mechanical properties and creep characteristics are strong functions of temperature. Note that the maximum hot-junction temperature does not exceed its established 1000°C limit, and that the 1172°C maximum capsule temperature is far below its established 1330°C limit. The reason why the capsule temperature is much lower in the Mars Rover RTG than in the Galileo RTG is the presence of helium inside the canister. Helium greatly reduces the internal temperature drops in the heat source module.

At the midplane of the RTG there are six temperature drops. The first (~85°C) represents the drops inside the heat source module, across the graphitics and helium gaps. The second (~29°C) is the drop across the helium gap to the canister, and the third (~62°C) is across the vacuum gaps and through the TE heat collectors. The fourth (703°) is the temperature drop across the SiGe TE legs. As can be seen, this is the largest of the drops. It is the only one that makes a useful contribution in actually generating electrical power. All the other temperature drops represent thermodynamic losses. The fifth drop (~29°C) represents the thermal resistance of the unicouple's cold-end and the loss for circumferential heat transport through the aluminum housing to the nearest fin; and the sixth drop (44°C) is that due to radial heat flow through the fin itself.

The full report [1] presents a detailed description and discussion of the axial variation of temperatures, heat flow rates, couple voltages, and efficiencies in the RTG. It also presents the integrated values of heat flows and efficiencies. The RTG has a material efficiency of 7.86%, a couple efficiency (after electrode and contact losses) of 7.52%, a converter efficiency (after thermal losses through the multifoil insulation) of 6.46%, and a system efficiency (after heat losses through the RTG ends) of 6.32%. Thus, there are substantial differences between the BOM material efficiency, couple efficiency, converter efficiency, and system efficiency. This highlights the importance of specificity in reporting RTG efficiencies.

7.2 ENVIRONMENTAL EFFECTS

The preceding results were for the beginning-of- mission performance of the radiatively cooled baseline RTG with a 300°K sink temperature. The same RTG was also analyzed for other environmental conditions, to determine. The effect of water-cooling versus radiation cooling, the effect of a cold Martian winter night (140°K) versus a hot summer day (300°K), and the effect of fuel decay and thermoelectric materials degradation during the four-year mission on the performance of the baseline RTG. Detailed results of these analyses are presented and discussed in the full report [1], and are summarized in the Results and Conclusions section of the present paper.

8.0 ALTERNATIVE RTG DESIGN

In addition to the baseline RTG, a number of alternative RTG designs were laid out and analyzed. These include the options of powering the Rover with four 125-watt RTGs instead of two 250-watt RTGs, the use of a variety of thermoelectric materials ranging from very conservative ($Z=0.00058K^{-1}$) to very optimistic ($Z=0.00140K^{-1}$), the use of half-length unicouples instead of standard-length unicouples, and the use of multicouples instead of unicouples. Descriptions of those design alternatives are presented in the full report [1]. Only the multicouple RTG will be described in the present paper.

8.1 Thermoelectric Multicouple: The standard multicouple, developed for DOE's MITG and Mod-RTG programs, is depicted in Figure 24. Its principal difference from the unicouple depicted in Figure 8 is that instead of two TE legs each thermoelectric element has 40 legs, which together with its hot and cold electrodes form 20 series-connected couples. The standard multicouple legs are only 0.3" long, compared to the unicouple's 0.8" leg length. This reduces the weight of the thermal insulation and of the RTG housing. Another major difference is that the multicouples tested to date had n-legs with a GaP additive. This leads to a significant increase in their figure of merit and efficiency.

Figure 24. Multicouple Cross-Section

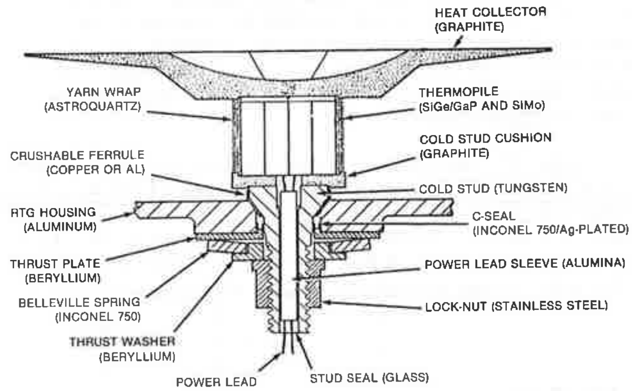

The multicouple's legs are bonded to and insulated from, each other by 0.002" glass layers. The heat collector, approximately 2" square, is made of graphite. In contrast to the unicouple, the multicouple's mounting stud and power leads penetrate through the RTG housing, and electrical connections between multicouples are made on the outside of the housing. As will be seen, these differences affect the Rover RTG design.

Multicouples operating at the required hot-junction temperature (1000°C) have a much smaller data base than unicouples, which have successfully operated for periods in excess of 100,000 hours. Multicouple development was initiated in the late 1970s [12], their present design was defined in 1983 [13], and their most successful test to date (of an assembly of eight multicouples produced at GE and tested at Fairchild) ran for 6000 hours, until it was interrupted for a planned modification of the test fixture and for withdrawal of three of the multicouples for destructive examination in late 1988. The test results indicated that multicouples can deliver stable performance with only modest degradation, at least for 6000 hours.

8.2 Multicouple RTG Design: A horizontal cross-section of an RTG employing standard-size multicouples is shown in Figure 25. The multicouple-RTG design is generally similar to the unicouple-RTG design shown in Figures 9 and 10, and only the significant differences will be mentioned.

As in the MITG and Mod-RTG designs, there are eight multicouples per horizontal layer, and only one multicouple layer per heat source module. For a 250-watt(e) power output, the RTG has 16 heat source modules. Thus, there are 128 multicouples per RTG, or about one fifth as many thermoelectric units as in the unicouple RTG.

Figure 25. Multicouple RTG, Horizontal Cross-Section

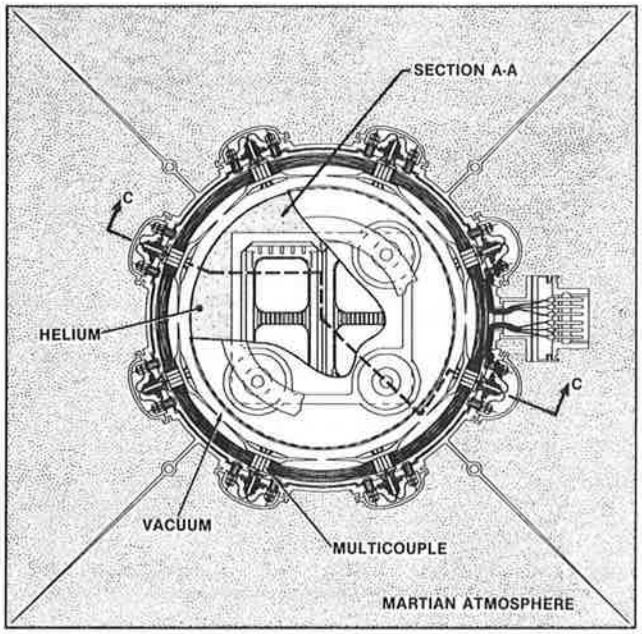

In the Mod-RTG the multicouple mounting holes are sealed by conical metal ferrules, but these would be inadequate for preventing inflow of the Martian atmosphere during long-term operations on Mars. Therefore, the bolt holes in the present design are hermetically sealed by eight semi-cylindrical aluminum seal covers welded to the aluminum housing hubs.

In the standard multicouple design, the leads pass through the housing wall, and are series-connected on the outside. To preserve hermeticity in the present RTG design, the series leads are passed back to the inside of the housing via insulated studs, for internal series connections between the eight multicouples in each ring.

As in the Mod-RTG, the eight multicouples are embedded in a 0.3″-thick layer of thermal insulation, consisting of 60 layers of 0.0003″-thick molybdenum foils, separated from each other by zirconia spacer particles. This type of insulation is not only lighter than the standard unicouple insulation, but its lower thickness also leads to significant weight saving due to the consequent reduction in housing diameter from 9″ to 7.5″.

The option shown in Figure 25 has four radiator fins. The alternative of eight (shorter and thinner) fins was also analyzed. The analytical results showed that the two options yield very similar specific powers.

As shown, the series connections between the multicouples are horizontal rather than vertical. The multicouple RTG design is modular [12], because each horizontal ring produces the desired RTG voltage (30V). The 16 rings are connected in parallel. To isolate the effect of shorts-to-ground, the leads from each of the sixteen current loops are separately brought out to the power conditioning unit through a multipin terminal near the base of the RTG, as shown at the right of the figure.

Detailed performance parameters of the multicouple RTG and of the other design alternatives are presented and discussed in the full Fairchild report [1]. A summary of the study's results and conclusions is presented below.

9.0 RESULTS AND CONCLUSIONS

1. The current multifoil-insulated GPHS-RTG and Mod-RTG designs can be modified to operate in an environment with an external atmosphere (e.g., Mars).
2. The helium generated by the fuel's alpha decay can be vented to the outside without intrusion of the external atmosphere into the RTG.
3. The use of novel selective vents and unproven high-capacity getters is not required.
4. The Rover RTGs can be built from safety-qualified General Purpose Heat Source modules and from performance-proven standard SiGe unicouples or SiGe/GaP multicouples.
5. Basic designs have been prepared for both unicouple RTGs and multicouple RTGs. These designs apply both to current TE elements and to elements of advanced designs and materials.
6. The baseline RTG containing 18 heat source modules and employing 576 standard unicouples has a mass of 58.7 kg, a length of 45.9 inches, a housing diameter of 9.1 inches, and a tip-to-tip radiator span of 15.2 inches.
7. At the beginning and end of the four-year mission on Mars, the baseline RTG has respective power outputs of 283 and 259 watts, system efficiencies of 6.44 and 6.08%, and specific powers of 4.82 and 4.41 watt/kg.
8. The modular heat source stack in the Rover RTG is held together by axial load springs, without the use of mid-span supports.
9. The springs will support and hold the heat source together under transverse loads of 25 G in the water-cooled RTG during Earth launch and Mars entry and 15 G in the radiation-cooled RTG during subsequent Mars operations, without exceeding the allowable stresses in the springs, the heat source, or the RTG housing.
10. In case of inadvertent reentry into the Earth's atmosphere, the RTG's aluminum housing will burn off, allowing the heat source modules to separate and impact at a relatively low velocity.
11. An auxiliary coolant loop (e.g., water) will be required to cool the RTG while it is within the Rover's aeroshell during launch and transit to Mars.
12. The RTG can deliver full operating power during its water-cooled cruise to Mars.
13. The power output of the radiatively cooled RTG is essentially independent of the Martian temperature.
14. The combined effect of fuel decay and thermoelectric material degradation during the four-year mission reduces the power output by 8%.
15. The RTGs are mounted on the Rover in a vertical orientation, to avoid the building of wind-borne Martian sand on its heat rejection surfaces.

16. Rover's 500-watt power requirement can be satisfied with two 250-watt or four 125-watt RTGs, with respective lengths of 45.9 and 26.7 inches. Both sizes appear to be compatible with currently envisaged Rover designs.

17. The mass of four 125-watt RTGs is 6% higher than that of two 250-watt RTGs. This disadvantage may be offset by their greater ease of integration with the spacecraft, and by the fact that - with four independent RTGs - failure of one would still permit continuing mission operation at 75% power.

18. If unicouples with SiGe/GaP legs were developed, they would raise the specific power of the RTG by 9.1% above that of the SiGe baseline design.

19. For the same thermoelectric material (SiGe/GaP) and the same thermal power, an RTG using short unicouples is 9.1% lighter than one using standard unicouples; but because of its doubled heat flux and current density and its resultant higher thermal and electrical contact losses, it produces 5.0% less power.

20. Because of their lower efficiency, short unicouples offer only a 5.0% specific-power improvement over standard-size unicouples.

21. A 250-watt RTG using standard SiGe/GaP multicouples is 23% lighter, 9.4% shorter, and 7% more efficient than the baseline RTG using standard SiGe unicouples.

22. The RTGs' fuel loading and mass can be significantly reduced by employing thermoelectric materials with much higher figures of merit, when these become available. As a highly optimistic example, if a standard-size unicouple with a figure of merit of $0.00140 K^{-1}$ were developed, it would reduce the baseline RTG's fuel loading by 46% and its mass by 37%.

The ultimate design and material selections will represent a trade-off between minimizing the RTG mass to help meet the Rover system design goals and minimizing the need for new technology to reduce the development cost and time and the programmatic risks.

REFERENCES

[1] A. Schock, et al, "Mars Rover RTG Study." Fairchild Report FSC-ESD-217-550, August 25, 1989.

[2] Statement before the Committee on Energy and Natural Resources, United States Senate by Dr. Robert Rosen, Sept. 13, 1988.

[3A] J.D. Bourke, J.H. Kwok, A. Friedlander, "Mars Rover Sample Return Mission." AIAA-89-0417, 27th Aerospace Science Meeting January 9-12, 1989, Reno, Nevada.

[3B] J.R. Casani and M.S. Reid, "JPL and Mars Exploration." 39th Congress of the International Astronautical Federation, held in Bangalore, India, 10-14 October 1988.

[4] G.L. Bennett, J.J. Lombardo and B.J. Rock, "Development and Use of Nuclear Power Sources for Space Applications." Journal of the Astronautical Sciences, Vol. XXXIX, Dec. 1981.

[5] J.T. Rose, "Conceptual Design of the Mars Rover Sample Return System." AIAA-89-0418, 27th Aerospace Science Meeting, January 9-12, 1989, Reno, Nevada.

[6] J. Randolph, "Mars Rover Sample Return Orbiter Design Concepts." AIAA-89-0421, 27th Aerospace Science Meeting, January 9-12, 1989, Reno, Nevada.

[7] T. Gamberk, L. Rogers, "Aerocapture, Entry and Landing Systems for the Mars Rover Sample Return." AIAA-89-0422, 27th Aerospace Science Meeting, January 9-12, 1989, Reno, Nevada.

[8] D. Pivirotto, T. Penn, W.C. Dias, "Mars Rover 1988 Concepts." AIAA-89-0419, 27th Aerospace Science Meeting, January 9-12, 1989, Reno, Nevada.

[9] "Environment of Mars, 1988", Jet Propulsion Laboratory, TM100470, Oct. 1988.

[10] A. Schock, "Design Evolution and Verification of the General Purpose Heat Source." Proceedings of the 1980 Intersociety Energy Conversion Engineering Conference, Volume 2, pages 1032-1042.

[11] G. Bennett, et al, "Update to the Safety Program for the General Purpose Heat Source Radioisotope Thermoelectric Generator for the Galileo and Ulysses Missions." Transactions of the Sixth Symposium on Space Nuclear Power Systems, Albuquerque, New Mexico, 8-12 January 1989.

[12] A. Schock, "Modular Isotopic Thermoelectric Generator." Proceedings of the 1981 Intersociety Energy Conversion Engineering Conference, Volume 1, pages 327-342.

[13] A. Schock, "Revised MITG Design, Fabrication Procedure, and Performance Predictions." Proceedings of the 1983 Intersociety Energy Conversion Engineering Conference, Volume 3.

[14] A.F. Ioffe, Semiconductor Thermoelements and Thermoelectric Cooling. Infosearch, London (1957).